Physical Sciences Section

Pakistan J. Sci. Ind. Res., Vol. 17, Nos. 4-5, August-October 1974

PARTICLE SIZE DETERMINATION BY LIGHT SCATTERING IN STREAMING SYSTEMS

NOOR AHMAD

Institute of Physical Chemistry, University of Peshawar, Peshawar

(Received January 23, 1974; revised June 24, 1974)

Abstract. Light scattering by nonspherical particles which are oriented by streaming, furnishes a method for investigating the size and shape of the scattering materials. A new experimental technique used for this investigation is the measurement of the change in the intensity of the light scattered by anisometric colloidal particles when they are oriented by a velocity gradient. The systems investigated consist of suspensions of β-FeooH crystals. The estimated lengths are found to be within the expected value as determined independently by electron microscopy.

The light scattering methods at rest are relatively insensitive to particle shape, since the effect observed at a given angle of observation, in a system at rest, is the average of all possible orientations of the nonspherical bodies with respect to the incident beam of radiation and the direction of observation. By this averaging, characteristic effects of nonspherical shape upon light scattering are lost. Therefore, light scattering studies on systems with oriented nonspherical scattering bodies are preferable whenever a reasonable degree of orientation is experimentally attainable without extraordinary difficulties.

The orientation of the particles can be achieved by applying an electric field, a magnetic field, or velocity gradient in laminar flow. Hydrodynamic orientation was selected in the present case. The theory of this type of orientation in three-dimensional system was developed by Peterlin and Stuart,[1] in extension of an earlier theory by Boeder[2] which was limited for a two-dimensional system. Because of the importance of the velocity gradient in hydrodynamic orientation, an experimental set up is desirable in which the gradient is constant, or nearly so, perpendicular to the direction of flow. This condition is fulfilled by the gap between two concentric cylinders of which one is rotating and the other is stationary. The theory of this arrangement for the case of stationary outer cylinder is due to Taylor.[3] It is this type of arrangement which was used in the present work.

By producing a velocity gradient across the annular space by rotating the inner cylinder of the concentric cylinder apparatus one tends to orient the particles in the direction of flow lines. Since the particles are of colloidal dimensions, they are also acted upon by the random forces of the rotatory Brownian motion which tends to upset the flow induced orientations. This opposing force is described by a rotational diffusion constant (D_r) which is a function of particle shape and size. At a given velocity gradient G, rotatory Brownian motion and the torque on the particle due to the velocity gradient balance out to produce an uneven rotation of the particle about its minor axis in which it spends more time at a certain preferred angle with respect to stream lines than at any other. The higher the velocity gradient, the longer period of time the particle will dwell at that angle and closer that angle will be to stream lines. The relationship between this preferred angle, velocity gradient, diffusion constant and axial ratio has been put on exact theoretical basis by Peterlin and Stuart.[1] Scheraga, Edsall and Gadd[4] have tabulated the values of extinction angle χ (the angle which characterizes the orientation of an anisometric particle with respect to the direction of the velocity gradient, and which is to be expected in terms of the axial ratio, p, and the parameter $\beta = G/D_r$. (It is in the experimental determination of this most preferred angle that light scattering differs from flow birefringence, although theories relating velocity gradients G to orientation and to the rotatory diffusion constant D_r are the same.) The angle of most preferred orientation is located by locating the angle at which most light is scattered. According to Gans[5] for prolate spheroids $p > 1$ (the shape assumed for β-FeooH crystals in this investigation).

$$D_r = (3KT)/(16\pi\eta_1 a^3)[p^4/(p^2-1)] \times [(2p^2-1)/(p\sqrt{p^2-1})] \times \ln[(p+\sqrt{p^2-1})-1]$$

Here K, Boltzman constant; T, absolute temperature; η_1, viscosity of the system; p, axial ratio; and a, is the length of the crystals.

After experimentally finding the value of D_r and taking the electron microscopic values of axial ratio p one can calculate the values of a.

Apparatus

The apparatus consists of (a) the concentric cylinder assembly, and (b) the optical system.

The Concentric Cylinder Assembly. The concentric cylinder assembly (Fig. 1) supported vertically

consists of two coaxial cylinders of which only the inner cylinder rotates. The annulus between the cylinders can be varied from 0.2 to 0.8 mm by suitable choice of the rotor (inner cylinder). This assembly, built almost entirely of stainless steel, has two openings (1, 2 in Fig. 1) parallel to the axis of cylinder unit, providing for the incident and trasmitted light beam through the annulus. A third main opening situated in the outer wall (3) allows for the measurements of the scattered light intensity of dispersed (or dissolved) solute in the annulus. The driving mechanism consists of a variable constant speed electronic drive controlling a motor equipped with a tachometer feed-back mechanism. Electronic drive attaches to a switch and variac, suitable gear reduction, from the motor to the driving pulley are also incorporated in the system. The transmission unit is a belt connecting the driving and rotor pulleys.

The Optical System. The optical system is described in Fig. 2. The light source (4) a water-cooled AH-6 mercury arc lamp is mounted vertically. The optical accessories are a collimating unit (lenses 5 and 6), a double slit (7) and two additional lenses (8, 9). Lenses (9) are actually a low-power microscope objective consisting of three small lenses. A nicol prism (10) is also housed in the holder of the lenses (9).

System Investigated

The slow hydrolysis of dilute, aqueous solutions of ferric chloride results in the formation of a positive lyophobic, colloidal solution containing β-FeooH crystals 6. The length and axial ratios of the β-FeooH crystals in a series of dilute aqueous solutions of ferric chloride, ranging from 23 to 77 mmoles, iron per liter, kept at room temperature, and aged for 130 days, showed unimodal frequency distribution and standard deviation of about 10%. The lengths of the crystals increase with increasing concentration, as do the axial ratios. Mean and modal lengths, and their axial ratios alongwith their standard deviation for the systems are given in Table 1 as obtained from electron micrographs.

Experimental Setup and Results

Figure 3 defines those symbols which pertain to the experimental variable involved in hydrodynamic orientation of spheroids.

$\vec{R}$, The incident beam. The axis of the concentric cylinder apparatus is parallel to $\vec{R}$. O the location of the solution or of the dispersed systems containing the light scattering bodies; $\vec{V}$ and $\vec{G}$, the direction of flow and of velocity gradient respectively.

$\gamma = 180° - \theta$; here θ is the angle of observation with respect to $\vec{R}$. φ is the angle between the symmetry axis of a single spheroid and inverse of $\vec{R}$; φ is the angle between the projection of the symmetry axis of a spheroid upon the $\vec{V}$—$\vec{G}$ plane and the direction of $\vec{G}$; and ω is the angle of observation

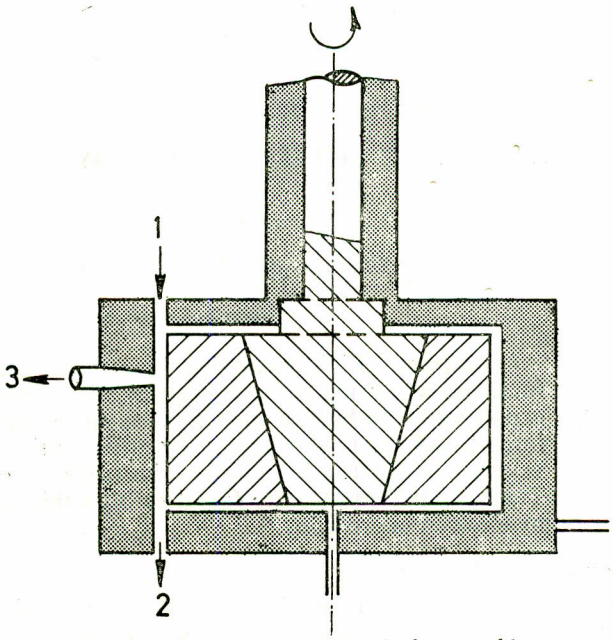

Fig. 1. The concentric cylinder assembly.

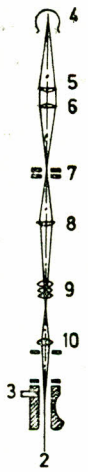

Fig. 2. The optical system.

with respect to $\vec{V}$ projected into the $\vec{V}$—$\vec{G}$ plane.

The light scattering measurements were done at $\theta = 90°$ of the incident light (Fig. 3). The angle ω was varied from 70 to 110° at an interval of 3–5°. The maximum shear rate used was of 1800/sec. All the measurements were done at fairly constant temperature of 24 ± 1°C. The gap width of the annulus used in these measurements was 0.639 mm. The concentration of the β-FeooH crystals was of the order 2–3 mg/100 g of dispersed system. An additional process was done for smaller particles. Smaller particles have a bigger rotary diffusion constant due to their large Brownian movements. In order to overcome this problem their viscosity was increased. This was accomplished with the addition of Carbowax (trademark for polyethylene compound 20 M linear of Union Carbide, New York). This was added into the first four systems investigated. The average size of these systems varied from 200 to 305 nm in length.

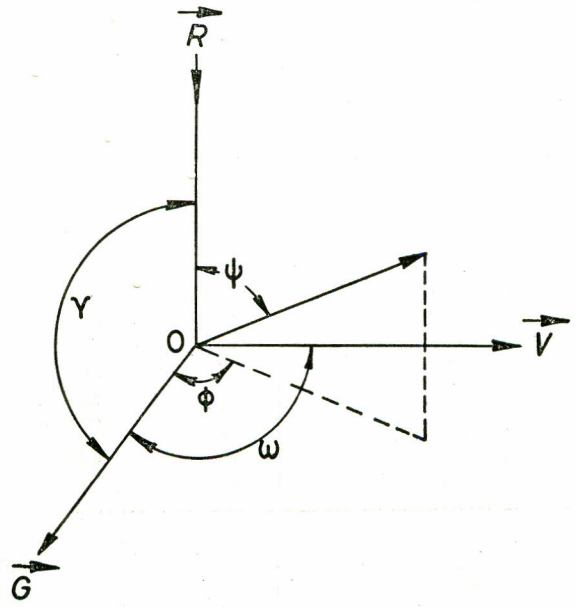

Fig. 3. Geometry of the flow arrangement considered.

Figure 4 represents the fractional increase in scattering due to hydrodynamic orientation in concentric cylinder apparatus. It gives the complete data only for 70 and 90°, while the average experimental curves are shown for $\omega = 80$, 100 and 110°. The concentration of the β-FeooH crystals was 2.05 mg/100 g of dispersed system. Open circles and triangles indicate systematic increase in shear rate while closed circles and triangles indicate the corresponding decrease in shear. The critical gradient for the system was calculated to be 1725/sec. The plot is for $\triangle I/I_R$ vs G, where

$$\left(\frac{\triangle I}{I_R}\right)_{\theta=90°;\,\omega} = \frac{(I_S)_G - (I_R)_{G=0}}{(I_R)_{G=0} - (I_W + I_{B.R.})_{G=0}}$$

$(I_S)_G$, intensity of the light scattered at a shear G; I_R, intensity of the light scattered by the system at rest; I_W, intensity of the light scattered by water at zero shear; and $I_{B.R.}$, intensity of the light scattered due to back reflection from the wall of the cylinder. Also $(I_W)_{G=0} = (I_W)_G$ because of the negligible change due to the scattered light intensity due to shear. and $(I_{B.R.})_{G=0}$ has been approximated to $(I_{B.R.})_G$ because of the unavailability of these values at different shear rates.

The bars represent the experimental uncertainty of the data. From a plot of fractional increase in intensity against different ω-values for particular shear rates, one can get the value of ω_{max}. The plot of χ vs G is shown in Fig. 5. Extinction angle, $\chi = \omega_{max} - 90°$, represents the angular position of an intensity minimum (in transmitted light) while ω_{max} defines the angular position of an intensity maximum (in laterally scattered light) which is experimentally easier to define. At the angle ($\omega_{max} - 90°$) one transverses a minimum of intensity while at ($\chi - 90°$) one transverses obviously, a second minimum, maxima being located at $\chi = \pm 45°$.

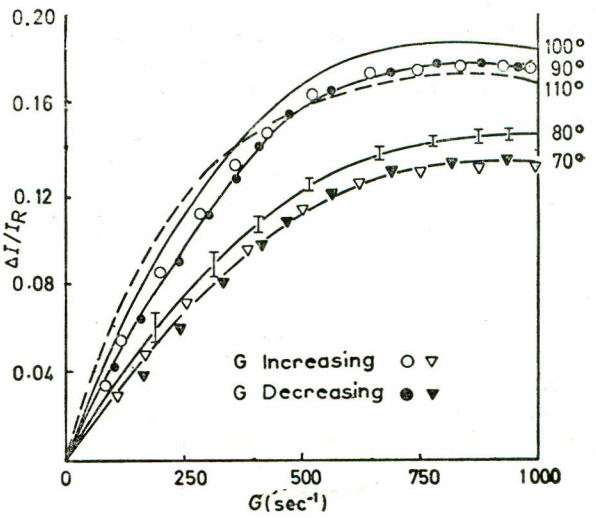

Fig. 4. Fractional hydrodynamic increase in scattering as a function of velocity gradient for system No. 6.

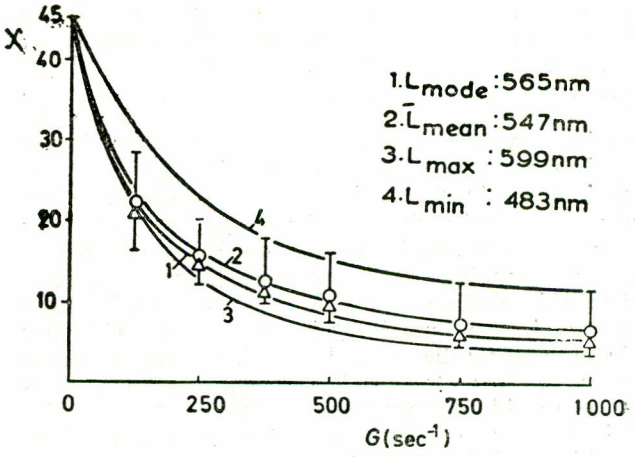

Fig. 5. X vs G values for system No. 6.

TABLE 1. MEAN AND MODAL LENGTHS AND AXIAL RATIOS ALONGWITH THEIR STANDARD DEVIATION (σ) AS DETERMINED BY ELECTRON MICROSCOPE. (β-FEOOH CRYSTALS TAKEN FROM SEDIMENT).

System	$L_{mean} \pm \sigma$	L_{mode}	$(a/b) \pm \sigma_{mean}$	$(a/b)_{mode}$
1	252± 37	236	4.2±0.5	4.05
2	217± 40	227	4.2±0.4	3.95
3	278± 48	318	4.7±0.4	4.7
4	321± 62	347	4.7±0.5	4.9
5	479± 91	552	4.9±0.6	5.2
6	474±102	565	4.8±0.7	5.6
7	427± 86	553	5.3±0.6	5.8
8	567±144	561	5.2±0.6	5.4
9	735±156	818	5.7±0.6	6.6
10	873±141	917	6.3±0.7	6.9
11	902±103	996	5.7±0.6	6.5
12	867±114	924	5.9±0.7	6.35

a, length in nm for the crystals; and b, widths in nm for the crystals.

Considering a prolate-spheroid, one will find that χ defines the most probable direction of its symmetry axis while ω_{max} defines the direction $\perp$ to it. Consequently χ decreases from a value of 45° as $\beta \to 0$ to 0° as $\beta \to \infty$, ($\beta = (G/D_r)$. While ω_{max} at the same time decreases from 135 to 90°.[7]

The bars in Fig. 5 represent the spread of the maximum, and also give the spread of the size of the system. Curve 1 gives the modal average of the system of 565 nm. The mean size of 547 nm is given by curve 2. Both of these, i.e. L_{mode} and L_{mean}, were obtained by electron microscopic measurements.

The maximum length of 599 nm is obtained by cruve 3 while curve 4 gives the minimum length of 483 nm.

L_{mean}, L_{max} and L_{min} of the twelve systems of β-FeooH crystals are given in Table 2.

TABLE 2. MEAN, MAXIMUM AND MINIMUM LENGTHS IN NM AS DETERMINED BY LIGHT SCATTERING FOR UNPOLARIZED LIGHT FOR THE TWELVE SYSTEMS.

System	L_{mean}	L_{max}	L_{min}
1	249	276	210
2	230	252	200
3	280	319	238
4	367	435	298
5	521	603	423
6	547	599	483
7	525	691	446
8	566	679	481
9	830	1077	689
10	955	1191	778
11	995	1238	829
12	940	1253	796

Discussion

Twelve different preparations of different length and axial ratios were used.

Figure 4 shows the variation of the flow induced fractional increase in light scattering with the velocity gradient G, on observing the very thin liquid layer, contained in 0.639 mm gap. Laminar flow produces a maximal fractional increase in scattering depending on the system being used, smaller for the small particle systems 1–4, and greater for the larger particle systems. This fractional increase reaches a maximum value for all the systems, and levels off for systems 1–4 with shear, while in the case of other systems is followed by a small decline at different G values depending on the system used. In some cases after this decline, there is sudden second sharp increase in the scattering in the range of higher G values below the critical velocity gradient where turbulent flow sets in. This strong effect in systems whose solid concentration was only $1\text{–}3 \times 10^{-3}$ weight per cent demonstrates the remarkably high sensitivity of the method to deviations in the shape of scattering object from spherical symmetry. The decline effect is due to the establishment of a centrifugal concentration gradient and it is found only with crystals of microscopic length ($> 0.5\ \mu$). The second more intriguing and more general effect could be traced to localized vortices. It is pronounced only at G values near G critical.

Similar shaped curves were obtained for a series of other ω-values than $\omega = 90°$ (the angles θ and φ being held constant at 90°). However, the numerical $(\triangle I/I_R)$ values, obtained at a given G, varied appreciably with ω. From a series of such measurements the $(\triangle I/I_R)$ vs ω 'angular spectrum' could be obtained. This function should and did exhibit a maximum at the ω-value at which observation is perpendicular to the most probable direction of orientation of the major axis. This characteristic ω-value which was within the experimentally accessible range of angles varied necessarily with G. Also the sharpness of the maximum increased at high shear rates. This variation and sharpness of the maximum is seen in Fig. 5 where the angle $\chi = \omega_{max} - 90°$ is used for the sake of easy comparison with streaming birefringence results. The agreement between calculated and most probable observed χ-values is seen to be fairly good. It will be noted, however, that the deviation between calculated and most probable observed χ-values varies systematically with G, the calculated values being too high at low G-values and too low at high velocity gradients. This can be easily understood as the result of the finite size distribution. It is, therefore, quite probable that a further increase in the precision of measurements might allow one to obtain not only the numerical values of length and widths of rigid particles of known basic shape and weight, but also their distribution curve on assuming that the axial ratio is, in a first approximation constant.

The results of sizes for all these systems (Table 2) have a remarkable agreement to those obtained by electron microscopy (Table 1).

References

1. A. Peterlin and H. A. Stuart, Z. Physik., **112,** 1, 129 (1939).
2. P. Boeder, Z. Physik., **75,** 258 (1932).
3. G.I. Taylor, Phil. Trans., **223/A,** 289 (1923); Proc. Roy. Soc., **102/A,** 541 (1923); Proc. Roy. Soc., **157/A,** 546 (1936).
4. H.A. Scheraga, J.T. Edsall, and J.O. Gadd, J. Chem. Phys., **19,** 9, 1101 (1951).
5. R. Gans, Ann. Physik., **486,** 628 (1929).
6. H. Zocher and W. Heller, Z. Anorg. Allg. Chem., **186,** 73 (1930).
7. See equation No. 18 of ref. No. 4.